EFDA-JET-CP(06)04-24

F. Piccolo, F. Sartori, L. Zabeo, E. Gauthier, F. Trohay
and JET-EFDA Contributors

Upgrade of the Power Deposition and Thermal Models for the First Wall Protection of JET with an ITER-like Be Combination of Wall

Upgrade of the Power Deposition and Thermal Models for the First Wall Protection of JET with an ITER-like Be Combination of Wall

F. Piccolo[1], F. Sartori[1], L. Zabeo[1], E. Gauthier[2], F. Trohay[3]
and JET-EFDA Contributors*

[1]UKAEA/Euratom Fusion Association, Culham Science Centre, Abingdon, OX14 3DB, UK.
[2]Association EURATOM-CEA, CEA-Cadarache, 13108 St. Paul-lez-Durance, France
[3]NSA University de Lyon, 69621 Villeurbanne, France
**See annex of J. Pamela et al, "Overview of JET Results",*
(Proc. 20th IAEA Fusion Energy Conference, Vilamoura, Portugal (2004).

Preprint of Paper to be submitted for publication in Proceedings of the
SOFT Conference,
(Warsaw, Poland 11th – 15th September 2006)

ABSTRACT.
At JET the increase of the additional heating power and the ITER-like first wall upgrade planned for 2008 with new Be wall and W divertor will require an improvement of the protection system in order to guarantee the integrity of the first wall. An accurate estimate of the power load and the temperature of the tiles during a discharge will become crucial to prevent damage to the structure. In that perspective the JET protection system (WALLS) has been improved and is in operation at JET. The plasma magnetic information and the input power to the plasma are used to evaluate the thermal load along the first wall. The evolution of the power distribution and tile temperature during and after a discharge are calculated by the system. Termination of the discharge is required if a thermal limit is reached or if a vulnerable area of the vessel is exposed to an excessive level of power. The calibration and validation of the algorithm have been performed comparing the model estimates with the temperature measurements provided by thermocouples and a new Infrared Camera (IR). This paper describes the structure of the WALLS algorithm. The models used to estimate the power distribution and the thermal diffusion are discussed, and the results obtained are compared to the IR camera measurements.

1. INTRODUCTION

H-mode high density highly shaped plasmas, which show improved stability characteristics and long confinement times, represent one of the most promising future plasma scenarios. The investigation of plasmas close to the ITER design values in ELMy H-modes has motivated the improvements to the JET divertor. The divertor modifications, together with the increased performance of the JET additional heating systems, and the perspective of a Beryllium wall and tungsten divertor in JET [1] have led to the re-design of the first wall protection system (WALLS [2]).

The improved protection system extends the range of protective actions resulting in an increase of the acceptable power load on the first wall components. The strike-point protections have been updated to account for changes in the divertor geometry and for the extended operational space needed for the new ITER-like plasma configurations. The power exhaust and deposition models have been substantially improved.

WALLS has been re-designed to be able to account for radiation, neutral beam shine through power, diamagnetic energy variations and to distribute the power on the tiles according to an exponential SOL (Scrape Off Layer) model [3].

An advanced tile thermal model which solves the diffusion equation is also being developed. The target is to correctly estimate the tile surface temperature, which is the limiting factor for a beryllium tile. Experimental data on the Inner Wall Guard Limiter tiles (IWGL) can now be collected as a result of the introduction of a new Infrared (IR) Camera diagnostic [4]. A few pulses have been analysed and the IR data has contributed to the tuning of the WALLS models.

2. OVERVIEW OF THE WALLS PROTECTION SYSTEM

During a JET pulse, WALLS monitors the thermal loads on the first wall components and initiates

appropriate protective actions if any of these exceeds its maximum rating. The protection action consists on a pulse termination request. The effect is that the additional heating systems reduce their output in a few hundred milliseconds and the plasma current starts to decrease one second later.

2.1 STRIKE-POINT PROTECTIONS

The JET ¯first wall has been progressively covered with more and more CFC (Carbon Fiber Composite) tiles over the last two decades. Nevertheless, only a few areas can withstand the concentrated energy flows associated with the strike points. For this reason one of the most important tasks is to verify that the strike points are kept within the appropriate areas of the divertor (on Figure 1 the tiles numbered 1,2,3,5,6,7,8). These areas have a high power handling capability, the remaining areas are not designed to handle significant power and are intended sacrificial protection for rare events.

The new High Field Gap Closure (HFGC) tile (on Figure 1 tile 0), was installed to protect internal cabling that would have been exposed to the plasma SOL if the location of the strike point was high on tile 1 as needed by the new configurations. Nevertheless an unprotected area was left at the gap between HFGC tile and the saddle coil protection tiles (shown on Figure 1) and for this reason WALLS limits the inner strike point position to be located anywhere on tiles 1,2 and 3.

While the latest protection guarantees a certain distance between the strike point and the unprotected gap, it is still possible, with a large flux expansion, that a significant amount of power can penetrate the gap between the HFGC tile and the saddle coil protection tiles (shown on Figure 1). Once fully commissioned, WALLS computes the ¯field line angles, poloidal and toroidal, calculates the power density and verifies that these parameters are within a safe operational range.

Most of the exhaust energy of JET is delivered to the outer strike point. In new configurations, with very high lower triangularity, this strike position is located on the new Load Bearing Septum Replacement Plate tile (LBSRP). While all the horizontal surfaces of the tile have good power handling capabilities, the vertical side and the area indicated by the number 4, are not designed to take significant power. WALLS restricts the outer strike point to the right of the LBSRP apex and the inner strike to the left of tile 4.

Between a tile and the next in the toroidal direction there is a finite gap which is inserted for mechanical and practical reasons. If the tile edges facing this gap are exposed to power flow, very high temperatures on the tile edge can be reached. The divertor tile surfaces have a toroidal inclination so that for typical plasmas the next tile edge is shadowed. This solution works for a limited range of angles in the inclination of the exhaust power flow relative to the tile surface. Too steep an angle will expose the tile edge, while too shallow an angle will mean that only part of the tile surface is wetted, resulting in a higher power density. WALLS enforces a different set of limits for this angle for each of the divertor tile faces.

The shape reconstruction is provided by the real time algorithm (FELIX, [5]) that by elaborating magnetic measurements is able to produce good estimates of the plasma-wall contact points and of the magnetic field structure near thefirst wall components.

2.2 ENERGY PROTECTION

Concerning the thermal load on first wall components, WALLS calculates the total energy deposition on the inner wall tiles (see Figure 2) and in the divertor region.

The tiles are made of CFC, a material which can withstand high power loads. However, the tiles are in contact with inconel components, which can with-stand limited thermal stresses before losing their mechanical properties. For this reason JET Operating Instructions impose a bulk temperature limit of 700 ±C. In fact, WALLS imposes an energy limit for each tile, where the threshold is obtained by multiplying the maximum tolerable temperature variation with the tile thermal capacity. The protection also accounts for the warming up of the tiles during a day of operation by varying the thresholds as function of the estimated inter-pulse cooling. The power exhaust model and the sharing algorithm are discussed in section 3.

An experimental protection algorithm based on an estimate of the tile temperature is also being developed. The model implements a linear finite difference solution of the heat diffusion equation. The aim is to have a more accurate description of the tile temperature profile which should allow a more relaxed set of operational limits. The planned introduction of a beryllium limiter, because of the relatively low melting temperature of the material, is a strong motivation for the activity. Details of the model can be found in section 4.

3. POWER EXHAUST AND DEPOSITION MODELS

The power deposition on the tile surface depends on the plasma exhaust power (Pexh), which is estimated by WALLS by considering the effects of the additional heating power, the plasma ohmic power, the neutral beam shine through power and the radiated power (bolometry). A simple schematic of the WALLS plasma exhausted power model is shown in figure 3.

The exhaust power is then distributed on the tile surfaces using the information from the SOL model.

The model for the power density Q in the scrape off® layer [3] considers the power density on the outboard midplane of the plasma as described by the equation:

$$Q\,(r) = \frac{P_{exh}}{2\pi\lambda r_b}\, e^{-\frac{r-r_b}{\lambda}}\,, \tag{1}$$

where r_b is the radius at the boundary on the mid plane, r is the disk radius at which the power density is computed and λ is the SOL thickness at the plasma outboard.

The total power deposited on a circular corona between r_b and r is computed by integrating equation (1). For values of $\lambda << r_b$ the integral becomes:

$$P\,(r) \cong P_{exh}\,(1 - e^{-\frac{r-r_b}{\lambda}})\,, \tag{2}$$

Because of the direct relationship between the power distribution and the flux surfaces, equation 2

can be rewritten as function of ψ. Assuming that at the mid-plane the vertical field B_v is almost constant for radial movements on the order of the SOL thickness λ, the following equation for the magnetic flux can be obtained:

$$\psi(r) = \psi_b + ((\delta r + r_b)^2 - r_b^2)\pi B_\upsilon \cong$$
$$\psi_b + 2\pi\delta r r_b B_\upsilon,$$

where $\delta r (<< r_b)$ is the considered radial movement within the SOL, ψ_b is the boundary flux and B_v is the vertical field at the outboard mid-plane. For small variation of r within the SOL region, the term $r - r_b$ can be substituted with the δr term in equation (2):

$$P(\psi) \cong P_{exh}\left(1 - e^{-\frac{\psi-\psi_b}{2\pi r_b B_\upsilon \lambda}}\right), \tag{3}$$

where P(ψ) is the power deposed on a tile surface in contact with flux lines from ψ to ψ_b. This equation can be applied to any first wall components delimited by two flux lines:

$$P = \left|(\psi_1) - (\psi_2)\right|,$$

where ψ_1 and ψ_2 are the magnetic fluxes calculated by FELIX at the tile edges ($\psi_b > \psi_1 > \psi_2$ and assuming that the normal field does not change direction along the component surface).

The power density is obtained by derivation of the equation (3):

$$Q(\psi) = \frac{P_{exh}}{2\pi\lambda r_b}\frac{B_n}{B_\upsilon} e^{-\frac{\psi-\psi_b}{2\pi r_b B_\upsilon \lambda}}, \tag{4}$$

where B_n is the normal component of the magnetic field.

The power deposition on the tile is function of the SOL thickness λ, which varies according to the plasma confinement mode (H-mode or L-mode), where the L-mode value for the SOL thickness is set to 1 cm, while it is set to 0.5cm for the H-mode case. At present no real-time H-mode/L-mode detector algorithm is implemented within WALLS, so the worst case scenario for each separate protection problem is always assumed.

A very limited power sharing among different machine areas is implemented. The total output power is applied unpartitioned at the same time at the divertor and the inner and outer limiters. The power ratio between outer and inner strike points is assumed to be 2.5:1.

4. TILE THERMAL MODEL

A model based on the integration of the power and the inter-pulse cooling provides only a rough estimate of the thermal stresses that the tile support elements are subjected to. In addition, the model does not provide a valid estimate of tile temperatures during the experiment. Not only the surface

temperature is severely under-estimated but also the temperature in some location in the divertor tiles that are currently instrumented with thermocouples is not correctly predicted.

A possible solution is the application of a semi-infinite tile analytical model. Unfortunately the complex shapes of both the divertor and the limiter tiles makes its application difficult. Moreover, real-time evaluation of the E_{rf} function [7] is not computational convenient.

For these reasons a finite difference model [6] of the thermal diffusion process has been developed. The tile parameters are kept constant, so that the final result is a set of linear ODEs which can be written in the form of state space equations and consequently reduced by model reduction techniques [8].

The model has been validated for a simple tile geometry by comparison with the analytical model. The results are shown in Figure 4 where first a constant power has been applied to the tile, and the tile is then left to cool.

A model has been produced only for the inner wall guard limiter tiles. The tile meshing with 1 cm elements is shown in Figure 5. A more refined model has also been used using 720 2.5mm elements. Applying a constant power profile to the first 6 elements of the tile surface and selecting the measurement points as indicated in the figure, the model reduction method was able to reduce the system to just 5 state variables. A model of this low complexity can be implemented for each tile in a different poloidal position of the JET first wall and can be executed in real-time using the currently available hardware (400Mhz processor) and timing requirements (10ms).

5. EXPERIMENTAL RESULTS

As a result of the installation of an IR camera facing the IWGL tiles, it has been possible to collect information about the behaviour of temperature of the tiles. Partially because of availability of the diagnostics and partially because of poor machine conditioning it has not been possible to perform successful dedicated experiment on the IWGL power load in order to validate the protection algorithms. During the experimental campaign it was possible to collect data during experiments that required heating a limiter plasma. The choice of plasma shape and power levels was not ideal for the purpose, but some information about the tiles was obtained. The limiter plasmas received 20MJ, 30MJ and 40MJ by neutral beam injection. The IR camera was set for optimal resolution at lower temperature (200−400 ±C) and the data acquisition was set for 10s at 1Hz.

The cooling time constant of the inner wall guard limiter tiles was identified experimentally by observing the temperature evolution measured by the IR camera after a JET pulse. The slow cooling time constant was also verified by comparing the model starting temperature for the next pulse with the actual temperature obtained by the IR data. An average of 15 minutes cooling time was found for all tiles. The cooling law seems to work consistently for all pulses in the set as shown in Figure 6 for one of the inner wall guard limiter tiles.

A second, faster time constant can be identified in the experimental data once the cooling evolution has been removed. Figure 7 shows the fit between this temperature re-equilibration time-constant and

the measured cooling curve. The time constant is roughly ≅ 30s. The finite difference model, described in section 4, agrees with the experimental data. It predicts not only a dominant re-equilibrating time constant of 30s but also a relative temperature evolution between points 1 and 5 of Figure 5 that substantially match the experimental data as shown in Figure 8.

On the other hand, the plasma exhaust and deposition modelling are in disagreement with the experimental result. While WALLS expects most of the 20-40MJ energy to have been loaded onto the IWGL, the IR camera temperature measurements show between 50% and 35% of the energy on the tiles. The measurement has been obtained by reading the IR data 1 minute after the pulse and correcting for the cooling since the additional heating was stopped. WALLS profile of energy deposition on the tiles is also quite different from that observed using the IR camera as shown figure 9. The difference can only be partially explained by an error in the scrape-off length or by the empirical weighting used to share power between tiles exposed to clock-wise and counter clock-wise energy °flows. Accounting for shadowing among the limiters and other components can probably produce better estimate.

CONCLUSION

This paper describes the new WALLS protection system that is being installed at JET. The new IWGL protection and the new strike point location limits have already been commissioned. The divertor energy limits, the strike points field line angles limits and the HFGC protection are planned to be installed in the late summer 2006.

One of the main problems left is to understand the disagreement in the tile power deposition shown by the IR data. Even if it might be possible to understand the problem in this special case, it must be accepted that a real-time calculation code will never be able to use all the diagnostic information and to model all the plasma phenomena related to the interaction with the walls. In fact, a protection system must choose an algorithm that is robust and that, in the worst case, over-estimates the monitored quantity.

The refined power deposition model in the new version of WALLS has allowed a total of 40MJ of energy in an inboard plasma before WALLS protective action was taken. This is in contrast to the 20MJ limit that would have been imposed by the previous version of WALLS.

The work on developing a WALLS protection system for the ITER-like first wall materials of JET has begun. The much reduced limits imposed by new beryllium tiles means that the real-time modelling of the plasma-wall interaction will have to be more accurate than at present. Good agreement between tile models and IR data is a good indicator that a way to model the tile temperature evolution might have been found once the thermal load is known.

ACKNOWLEDGEMENTS

The authors thank P. Andrews and G. Arnoux for providing the IR camera data, V. Riccardo for the tile data and P.J. Lomas for valuable discussions about inner wall protection. This work was performed under the European Fusion Development Agreement as part of an Enhancement project and was

partly funded by UK Engineering and Physical Sciences Research Council and by the European Communities under the contract of Associations between EURATOM and UKAEA. The views and opinions expressed here in do not necessarily reflect those of the European Commission.

REFERENCES

[1]. I. Nunes, et al., "Optimization of the JET Beryllium tile profile for power handling" this conference.

[2]. A. Cenedese, et al., "JET ¯first wall and divertor protection system", Fusion Engineering and Design 66-68 (2003), 785-790.

[3]. J. Wesson: "Tokamaks", Plasma wall interaction, 424-426.

[4]. E. Gauthier et al., Proceedings of the EPS 2005.

[5]. L. Zabeo, et al., "A new approach to the solution of the vacuum magnetic problem in fusion machines", this conference.

[6]. Niels Ottosen and Hans Pettersson, "Introduction to the Finite Element Method", 1992, Prentice Hall

[7]. Milton Abramowitz and Irene A. Stegun, eds. "Handbook of Mathematical Functions with Formulas, Graphs, and Mathematical Tables" New York: 13 Dover, 1972.

[8]. K. Zhou, J. C. Doyle, and K. Glover, "Robust and Optimal Control" New Jersey: Prentice Hall, 1996.

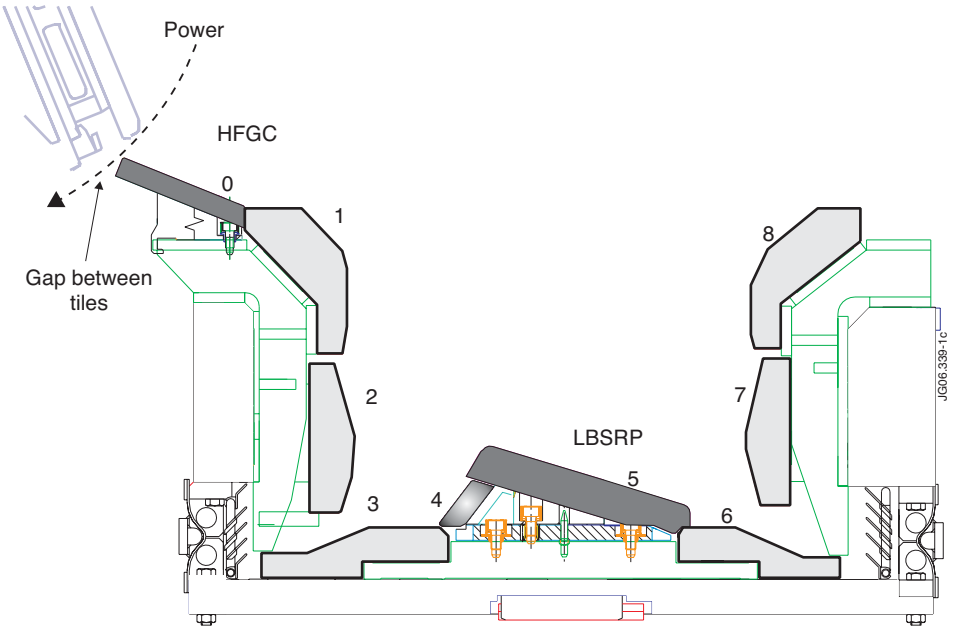

Figure 1: The new JET divertor configuration. The Load Bearing Septum Replacement Plate (LBSRP) and the High Field Gap Closure (HFGC) tiles are highlighted. The tile numbers are referred to in the text.

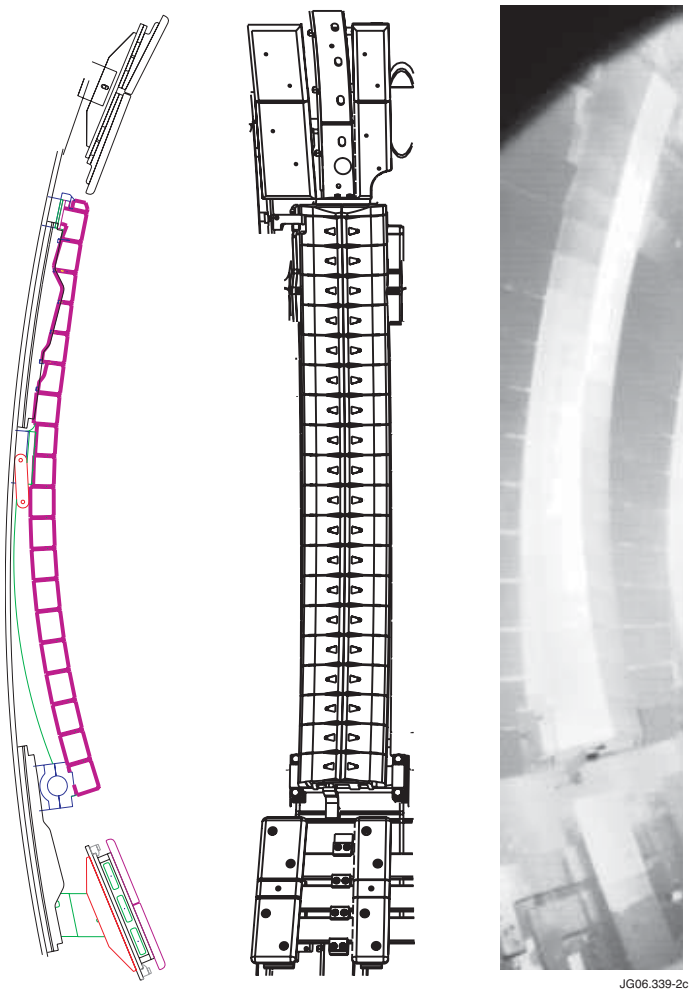

Figure 2: Inner Wall Guard Limiter. The Inner wall guard limiter tiles section and front view. The IR view of the inner wall tiles after a JET pulse. The shadowing effect of other limiters can be seen by observing that the top right and the bottom left regions of the guard limiter have higher temperatures.

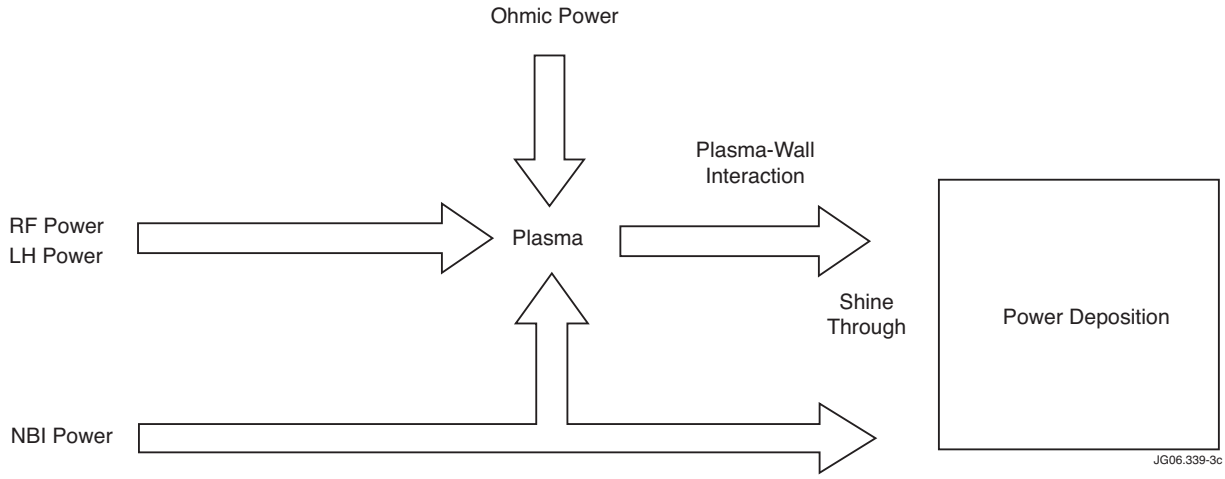

Figure 3: Power balance to compute the power deposition on the first wall. $P_{exh} = (P_{ohm}+P_{rf}+P_{lh}+P_{nbi}-P_{shine}-P_{rad})$, *where Pohm is the ohmic power,* P_{rf} *is the ICRH power,* P_{lh} *is the LHCD power, Pnbi is the neutral beam power, Pshine is the NBI shine through power, and Prad is the radiated power.*

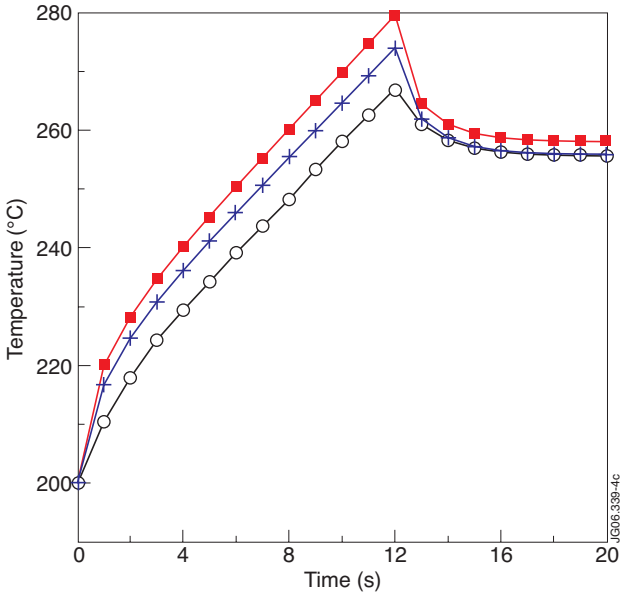

Figure 4: The analytical model (–) vs the finite difference model with 10mm (–o–) and 2.5mm (–+–) square elements. The difference is a function of the power density and can be considered equivalent to a delay in the response of the discrete model.

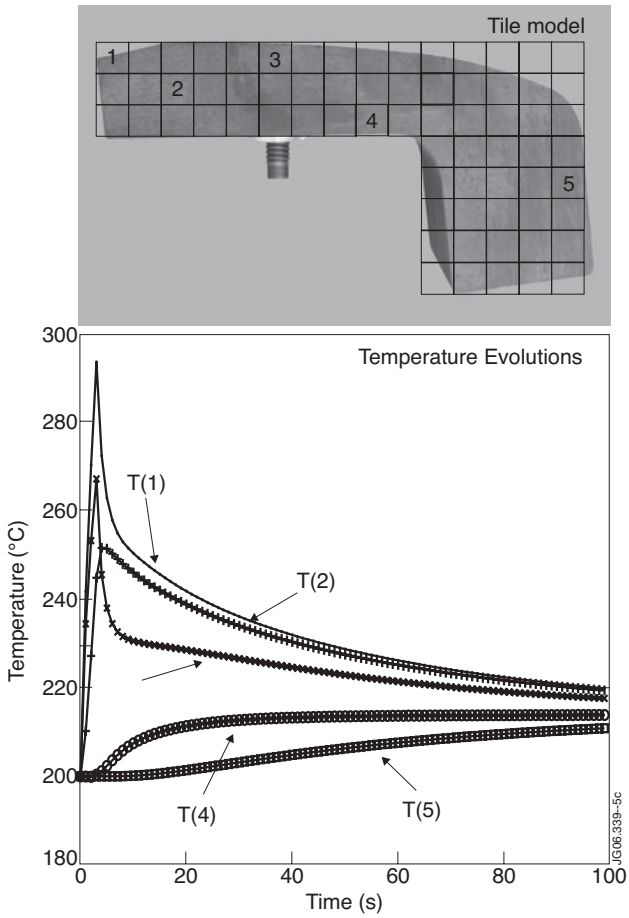

Figure 5: The upper ¯figure shows the tile model used for the Finite Difference Technique compared to the real tile. The numbers within the model are used in the lower figure to describe the temperature evolution as estimated by the model. The temperature excursion has been obtained by heating the first 6 elements on the tile surface (in figure from 1 to 3) with a square waveform of 5KW of power for 3s.

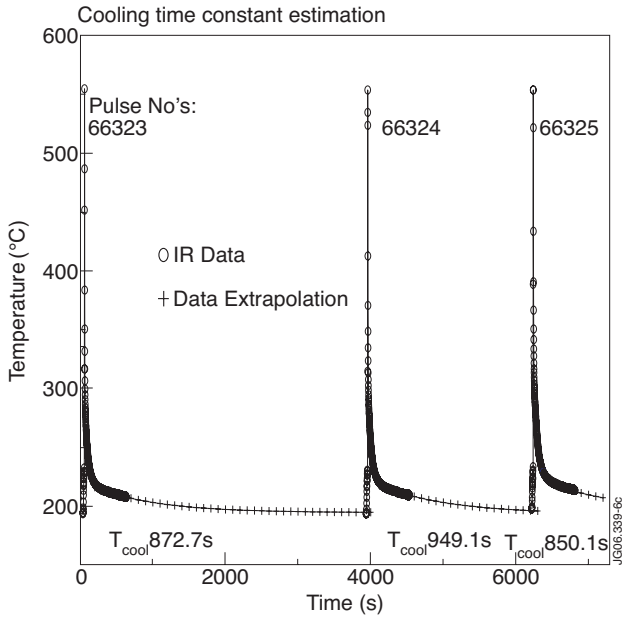

Figure 6: Estimate of the slow time cooling constant for one inner guard limiter tile. The cooling time constant (× lines) has been extrapolated to the IR camera data (o lines) so as to match the last few minutes of the time decay and the starting temperature of the next pulse.

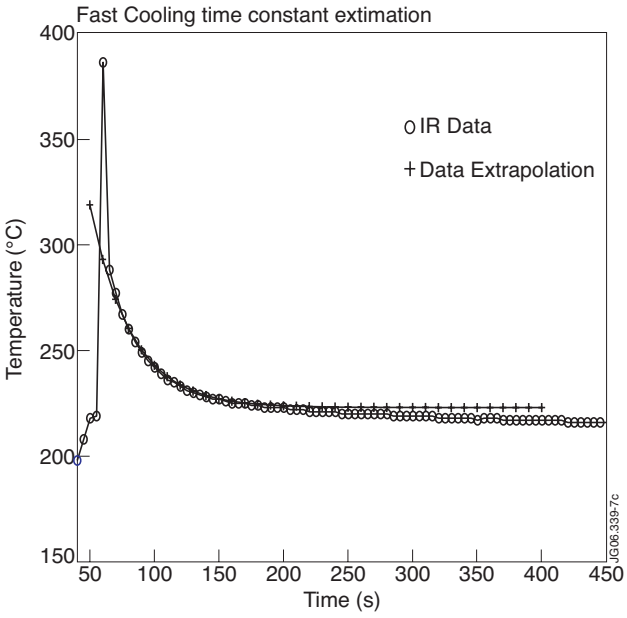

Figure 7: Fast cooling time constant estimate. The Figure shows the 30s time-constant exponential curve obtained by fitting to the tile surface temperature re- ported by the IR diagnostic. The result matches well with the data between 15–100s after the end of the additional heating.

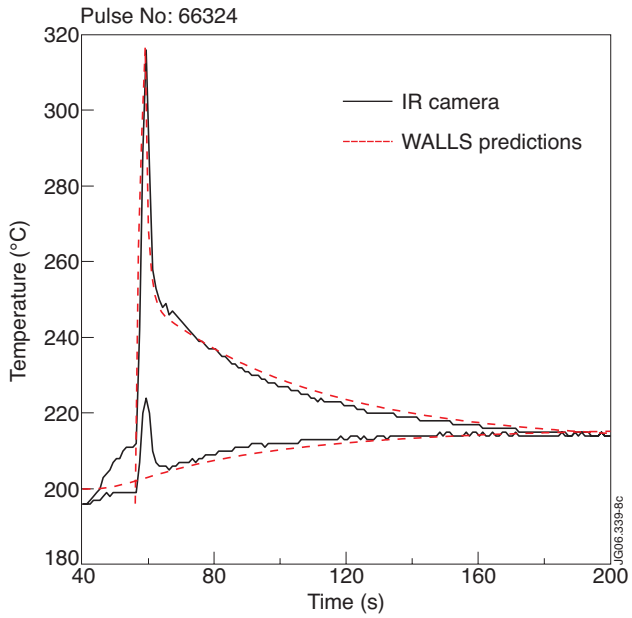

Figure 8: Comparison between experimental data and the model prediction of the temperature between points 1 and 5 of Figure 5. The input power on the tile has been set using the WALLS algorithm weighted down in order to fit the total energy (20KJ) measured using the IR camera.

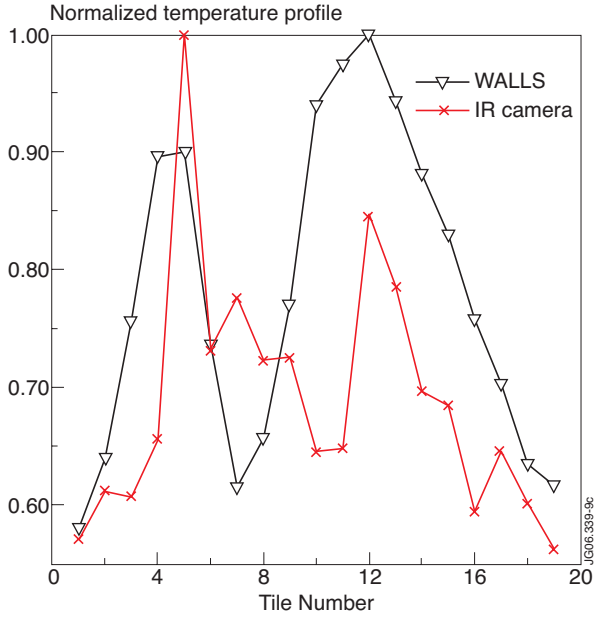

Figure 9: Normalized temperature profile on the Inner Wall Guard Limiter. The figure compares the normalized temperature profile as estimated by WALLS and as measured by the IR camera. A similar two-peak profile is observed even if the point temperature measurements do not agree.